Research Article | Vol. 24, No. 24 | 28 Nov 2016 | OPTICS EXPRESS 27536

Optics EXPRESS

Energy level systems and transitions of Ho:LuAG laser resonantly pumped by a narrow line-width Tm fiber laser

HAO CHEN,[1,7] TING ZHAO,[2] HAO YANG,[1] LE ZHANG,[1,3] TIANYUAN ZHOU,[1,4] DINGYUAN TANG,[1] CHINGPING WONG,[3] YUNG-FU CHEN,[5] AND DEYUAN SHEN[1,6,8]

[1]*Jiangsu Key Laboratory of Advanced Laser Materials and Devices, School of Physical Science and Electronic Engineering, Jiangsu Normal University, Xuzhou, Jiangsu 221116, China*
[2]*School of Electronic Engineering, Nanjing Xiaozhuang University, Nanjing, Jiangsu 211171, China*
[3]*School of Materials Science and Engineering, Georgia Institute of Technology, Atlanta, 30332, USA*
[4]*College of Materials Science and Engineering, Nanjing Tech University, Nanjing 210009, China*
[5]*Department of Electrophysics, National Chiao Tung University, Hsinchu 30010, Taiwan*
[6]*Key Laboratory of Micro and Nano Photonic Structures (Ministry of Education), Department of Optical Science and Engineering, Fudan University, Shanghai 200433, China*
[7]*chenhao@jsnu.edu.cn*
[8]*shendy@fudan.edu.cn*

Abstract: We presented a Ho:LuAG ceramic laser in-band pumped by a narrow emission line-width Tm fiber laser at 1907 nm. All of potential transitions between $^5I_7$ and $^5I_8$ manifold were discussed to form the Ho's in-band-pump energy level systems, which were not described in details earlier. For the emission band centered at ~2095 nm, both laser absorption and emission transition separately consisted of two groups were first analyzed and observed. Using output couplers (OCs) with different transmittances (T = 6, 10 and 20%), the similar ~0.5 W continuous-wave (CW) output power under an incident pump power of ~4.9 W was obtained, with twin (or triplet) emission bands respectively. The blue shift of center emission wavelengths was observed with the increase of transmittances.

OCIS codes: (140.3460) Lasers; (140.5680) Rare earth and transition metal solid-state lasers; (160.5690) Rare-earth-doped materials.

References and links

1. L. S. Rothman, I. E. Gordon, R. J. Barber, H. Dothe, R. R. Gamache, A. Goldman, V. I. Perevalov, S. A. Tashkun, and J. Tennyson, "HITEMP, the high-temperature molecular spectroscopic database," J. Quant. Spectrosc. Radiat. Transf. **111**(15), 2139–2150 (2010).
2. L. S. Rothman, I. E. Gordon, A. Barbe, D. C. Benner, P. F. Bernath, M. Birk, V. Boudon, L. R. Brown, A. Campargue, J.-P. Champion, K. Chance, L. H. Coudert, V. Dana, V. M. Devi, S. Fally, J.-M. Flaud, R. R. Gamache, A. Goldman, D. Jacquemart, I. Kleiner, N. Lacome, W. J. Lafferty, J.-Y. Mandin, S. T. Massie, S. N. Mikhailenko, C. E. Miller, N. Moazzen-Ahmadi, O. V. Naumenko, A. V. Nikitin, J. Orphal, V. I. Perevalov, A. Perrin, A. Predoi-Cross, C. P. Rinsland, M. Rotger, M. Šimečková, M. A. H. Smith, K. Sung, S. A. Tashkun, J. Tennyson, R. A. Toth, A. C. Vandaele, and J. Vander Auwera, "The HITRAN 2008 molecular spectroscopic database," J. Quant. Spectrosc. Radiat. Transf. **110**(9–10), 533–572 (2009).
3. K. Scholle, E. Heumann, and G. Huber, "Single mode Tm and Tm, Ho:LuAG lasers for LIDAR applications," Laser Phys. Lett. **1**(6), 285–290 (2004).
4. J. D. Kmetec, T. S. Kubo, T. J. Kane, and C. J. Grund, "Laser performance of diode-pumped thulium-doped $Y_3Al_5O_{12}$, $(Y, Lu)_3Al_5O_{12}$, and $Lu_3Al_5O_{12}$ crystals," Opt. Lett. **19**(3), 186–188 (1994).
5. T. Zhao, Y. Wang, D. Shen, J. Zhang, D. Tang, and H. Chen, "Continuous-wave and Q-switched operation of a resonantly pumped polycrystalline ceramic Ho:LuAG laser," Opt. Express **22**(16), 19014–19020 (2014).
6. A. Word-Daniels, A. Newburgh, A. Michael, L. Merkle, and M. Dubinskii, "Comparative of Ho^{3+} doped Yttria, LuAG and YAG as gain media for eye-safe resonantly pumped lasers," Proc. SPIE **7686**, 76860F (2010).
7. T. Zhao, D. Y. Shen, H. Chen, X. F. Yang, X. D. Xu, D. H. Zhou, and J. Xu, "Tm:fiber laser in-band pumped Ho:LuAG laser with over 18 W output at 2124.5 nm," Laser Phys. **21**(11), 1851–1854 (2011).
8. H. Yang, L. Zhang, D. Luo, X. Qiao, J. Zhang, T. Zhao, D. Shen, and D. Tang, "Optical properties of Ho:YAG and Ho:LuAG polycrystalline transparent ceramics," Opt. Mater. Express **5**(1), 142–148 (2015).

#274767 http://dx.doi.org/10.1364/OE.24.027536
Journal © 2016 Received 30 Aug 2016; revised 4 Nov 2016; accepted 13 Nov 2016; published 17 Nov 2016

Optics EXPRESS

9. B. Q. Yao, Z. Cui, X. M. Duan, Y. Z. Yang, Y. Q. Du, J. H. Yuan, and Y. J. Shen, "Passively q-switched ho:Luag laser with near-diffraction-limited beam quality," Appl. Phys. B **118**(2), 235–239 (2015).
10. Z. Cui, X. M. Duan, B. Q. Yao, H. Y. Yang, J. H. Yuan, C. L. Zhang, and T. Y. Dai, "Actively mode-locked Ho:LuAG laser at 2.1 μm," Appl. Phys. B **121**(4), 421–424 (2015).
11. Y. L. Tang, L. Xu, M. J. Wang, Y. Yang, X. D. Xu, and J. Q. Xu, "High-power gain-switched Ho:LuAG rod laser," Laser Phys. Lett. **8**(2), 120–124 (2011).
12. B. M. Walsh, "Review of Tm and Ho materials; spectroscopy and lasers," Laser Phys. **19**(4), 855–866 (2009).
13. N. P. Barnes, F. Amzajerdian, D. J. Reichle, W. A. Carrion, G. E. Busch, and P. Leisher, "Diode pumped Ho:YAG and Ho:LuAG lasers, Q-switching and second harmonic generation," Appl. Phys. B **103**(1), 57–66 (2011).
14. T. Zhao, F. Wang, and D. Y. Shen, "High-power Ho:YAG laser wing-pumped by a Tm:fiber laser at 1933 nm," Appl. Opt. **54**(7), 1594–1597 (2015).
15. B. M. Walsh, G. W. Grew, and N. P. Barnes, "Energy levels and intensity parameters of Ho^{3+} ions in $Y_3Al_5O_{12}$ and $Lu_3Al_5O_{12}$," J. Phys. Chem. Solids **67**(7), 1567–1582 (2006).
16. C. Cex, C. X. X. Cl, M. Zhuravleva, I. K. Yang, H. Rothfuss, C. L. Melcher, and S. Member, "Crystal Growth and Scintillation Properties of," IEEE Nucl. Sci. Symp. Conf. Rec. **7**(5), 1296–1299 (2010).
17. Y. Kuwano, K. Suda, N. Ishizawa, and T. Yamada, "Crystal growth and properties of (Lu,Y)3Al5O12," J. Cryst. Growth **260**(1–2), 159–165 (2004).
18. G. Rustad and K. Stenersen, "Modeling of laser-pumped Tm and Ho lasers accounting for upconversion and ground-state depletion," IEEE J. Quantum Electron. **32**(9), 1645–1655 (1996).
19. D. Y. Shen, H. Chen, Y. Wang, J. Zhang, and D. Y. Tang, "High power Tm:Fiber laser and in-band pumped Ho-doped ceramic lasers," in *2013 Conference on Lasers and Electro-Optics Pacific Rim*, (Optical Society of America, 2013), paper ThA1_1.
20. T. Zhao, H. Chen, D. Shen, Y. Wang, X. Yang, J. Zhang, H. Yang, and D. Tang, "Effects of Ho^{3+}-doping concentration on the performances of resonantly pumped Ho: YAG ceramic lasers," Opt. Mater. **35**(4), 712–714 (2013).
21. P. A. Budni, M. L. Lemons, J. R. Mosto, and E. P. Chicklis, "High-power/high-brightness diode-pumped 1.9-μm thulium and resonantly pumped 2.1-μm holmium lasers," IEEE J. Sel. Top. Quantum Electron. **6**(4), 629–635 (2000).
22. Z. Cui, B.-Q. Yao, X.-M. Duan, Y.-Y. Li, J.-H. Yuan, and T.-Y. Dai, "A graphene saturable absorber for a Tm : YLF pumped passively Q-switched Ho : LuAG laser," Optik (Stuttg.) **127**(5), 3082–3085 (2016).
23. H. Chen, D. Y. Shen, X. D. Xu, T. Zhao, X. F. Yang, D. H. Zhou, and J. Xu, "High-power 2.1 μm $Ho:Lu_{1.5}Y_{1.5}Al_5O_{12}$ laser in-band pumped by a Tm fiber laser," Laser Phys. Lett. **9**(1), 26–29 (2012).
24. D. H. Zhou, X. D. Xu, D. Y. Shen, D. Z. Li, J. Q. Di, C. T. Xia, F. Wu, and J. Xu, "Laser performance of holmium-doped $Lu_3Al_5O_{12}$ and $(Lu,Y)_3Al_5O_{12}$ crystals pumped by Tm:fiber laser," Laser Phys. **21**(11), 1876–1879 (2011).
25. H. Chen, D. Shen, J. Zhang, H. Yang, D. Tang, T. Zhao, and X. Yang, "In-band pumped highly efficient Ho:YAG ceramic laser with 21 W output power at 2097 nm," Opt. Lett. **36**(9), 1575–1577 (2011).
26. D. N. Patel, B. R. Reddy, and S. K. Nash-Stevenson, "Spectroscopic and two-photon upconversion studies of Ho^{3+}-doped $Lu_3Al_5O_{12}$," Opt. Mater. **10**(3), 225–234 (1998).
27. W. Liu, Y. L. Ju, T. Y. Dai, Z. Cui, J. Wu, B. Q. Yao, X. M. Duan, Y. J. Shen, and Y. Z. Wang, "Single-longitudinal-mode Ho:LuAG laser at 2.1 μ m," Laser Phys. **26**(2), 025002 (2016).
28. D. C. Brown, V. Envid, and J. Zembek, "Ho:YAG absorption cross sections from 1700 to 2200 nm at 83, 175, and 295 K," Appl. Opt. **51**(34), 8147–8158 (2012).

1. Introduction

~2 μm laser systems offer exceptional advantages in numerous applications, including remote sensing, medicine, and mid-infrared generation via pumping of optical parametric oscillators. In particular, LIDAR (light detection and ranging) laser mainly consists of a high power Q-switched solid-state laser in this range due to atmospheric transmission window dominated by the absorption lines of H_2O and CO_2 [1,2]. In this wavelength range, relatively small changes can cause dramatic changes in the effective range of LIDAR system [3,4], making the emission width of the laser material be a very important parameter.

With regards to Ho^{3+}-doped crystals, $Ho:Y_3Al_5O_{12}$ (Ho:YAG) and $Ho:Lu_3Al_5O_{12}$ (Ho:LuAG) have been studied well [5–15]. LuAG is an isomorphism to YAG, and both of them are oxide crystals with cubic garnet structure, and the lattice constant of YAG (12.0075 Å) is slightly larger than that of LuAG (11.9164 Å) [15–17]. When Ho^{3+} ions are doped into the host crystals, the crystal field will become larger due to the tighter lattice of Ho:LuAG compared to Ho:YAG. The larger crystal field enhances the Stark effect of Ho^{3+} ions and results in different thermal populations of the upper and lower levels at ~2.1 μm. Ho:LuAG lasers will have a slightly reduced lower laser thermal population than Ho:YAG.

Optics EXPRESS

Unfortunately, Ho:LuAG has no absorption bands in the 780-790 nm range, so it cannot be pumped directly by the commercially available high-power diode lasers. Co-doping of Tm^{3+} circumvents this problem, but leads to strong cross-relaxation and cooperative up-conversion losses. In high power laser applications, these will significantly increase the thermal loading and reduce the effective upper level lifetime [12,18–20]. Due to very low quantum defect, in-band pumping (resonant pumping $^5I_8 \rightarrow {}^5I_7$) with Tm-doped solid state lasers [9,11,21,22], Tm fiber lasers [5,7,8,10,14,23,24] and 1.9 μm diode lasers [13] can overcome the energy-sharing problem in the Tm and Ho co-doped system, improve the slope efficiency, reduce the waste heat and encourage the good beam quality. In this paper, Ho:LuAG ceramic laser resonantly pumped by a Tm fiber laser was presented. The tunable Tm fiber with a volume Bragg grating (VBG) was wavelength-locked at ~1907 nm, which had been used in our early Ho:YAG ceramic laser experiments [23,25]. Several recent publications about the Ho:LuAG laser materials, including single crystals grown by the Czochralski method [16,17] and ceramics fabricated by a reactive sintering method under vacuum [5,8], have been presented. Thermal properties, refractive indices, up-conversions [26], absorption and stimulated emission spectra of these laser materials have been described well. Continuous-wave (CW), Q-switched and actively mode-locked operations of Ho:LuAG laser have also been reported [5,8–10,22,27].

In these papers, for Ho:LuAG laser, the wavelengths of ~2077, ~2093, ~2095, ~2101, ~2125 and ~2131 nm have been achieved but jumped under different laser operating conditions. This wavelength shifts problem will bring us some troubles in some applications needing wavelength fixed. In [13], Barnes et al. have shown laser wavelengths could be predicted from the losses and the Ho concentration length product (product of the Ho concentra- tion and the length of the Ho:YAG ceramic sample). However, the interpretation of the wavelength shifts problem is principal and general terms. In fact, we think the energy level system is also a very key factor because it will determine how the Ho ions are excited and how the laser operates. We should make clear how the transitions perform between energy levels, so that we can control and achieve the wavelength we need. Following the earlier outstanding research, we had studied the potential transitions to form the level systems of Ho:LuAG.

We found the round-trip loss of a continuous-wave Ho:LuAG laser would dominate the laser wavelength shift, including the intrinsic loss, mirror transmissions, and even insertion losses of some optical elements when the Ho concentration length product has been fixed in a Ho:LuAG laser. The larger loss would give the Ho laser a chance to emit a shorter wavelength because the higher levels of $^5I_7$ manifold would be excited to act as upper laser levels. We also deduced the emission band centered at ~2095 nm consists of 2 groups of transitions with a slight wavelength difference. The 2 groups of transitions corresponded to 2 groups of laser energy level systems shown in the later which had different Stark splitting upper and lower energy levels, and they would show different laser performances. Using an uncoated Ho:LuAG laser ceramic material to introduce a large insertion loss, we observed the wavelength shifts among ~2095, ~2101 and ~2124 nm with output couplers (OCs) of different transmissions. And we also observed the slight wavelength shift around ~2095 nm as we have discussed. This work proved that forming and exciting a correct level system would help us to obtain an expected laser wavelength in an in-band-pumped Ho laser.

2. Spectroscopy and potential wavelengths

The absorption and emission spectra shown in Fig. 1 provided a research summary of the work done by Walsh [15], Daniels [6], Brown [28] and Yang [8], et al.. In this work, the absorption band from ~1900 to 1934 nm can be divided into two parts: one part is from ~1900 to 1918 nm (I) and the other from 1918 to 1934 nm (II). The emission spectrum from ~2085 to 2150 nm can be divided into 4 parts: ~2085 to 2098.4nm (III), 2098.4 to 2116.5 nm (IV),

Optics EXPRESS

2116.5 to 2128.9 nm (V) and 2128.9 to 2150 nm (VI). The most intense peaks are 2094.5, 2101.0, 2124.7 and 2130.0 nm respectively.

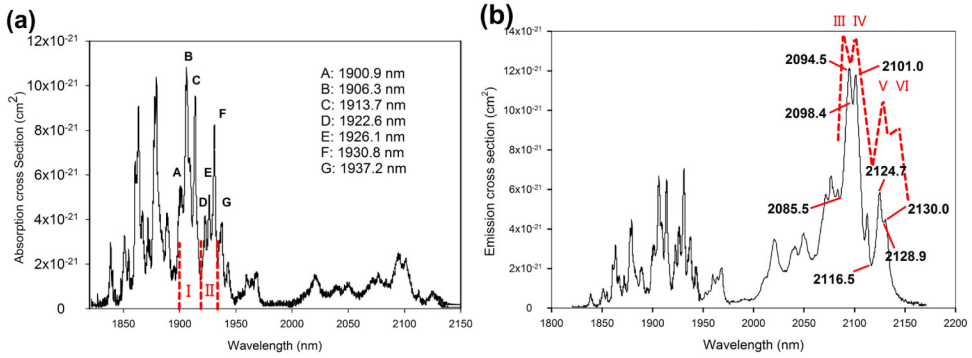

Fig. 1. Ho:LuAG absorption (a) and emission (b) cross sections @300 K [6]

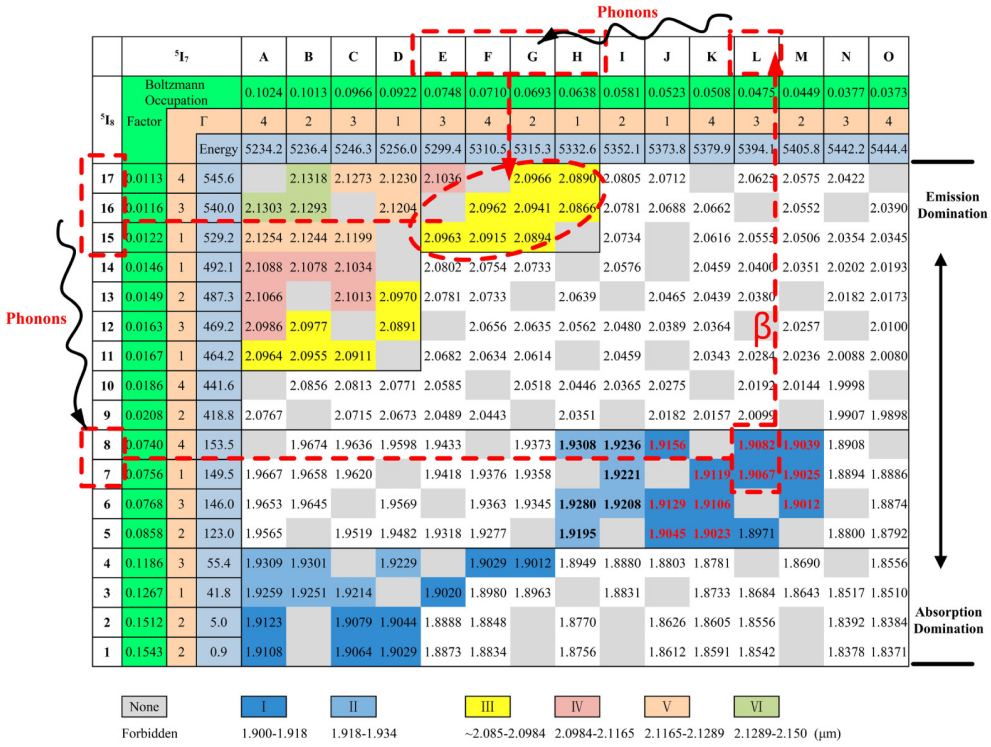

	$^5I_7$			A	B	C	D	E	F	G	H	I	J	K	L	M	N	O
	Boltzmann Occupation			0.1024	0.1013	0.0966	0.0922	0.0748	0.07101	0.0693	0.0638	0.0581	0.0523	0.0508	0.0475	0.0449	0.0377	0.0373
$^5I_8$	Factor	Γ		4	2	3	1	3	4	2	1	2	1	4	3	2	3	4
			Energy	5234.2	5236.4	5246.3	5256.0	5299.4	5310.5	5315.3	5332.6	5352.1	5373.8	5379.9	5394.1	5405.8	5442.2	5444.4
17	0.0113	4	545.6		2.1318	2.1273	2.1230	2.1036		2.0966	2.0890	2.0805	2.0712		2.0625	2.0575	2.0422	
16	0.0116	3	540.0	2.1303	2.1293		2.1204		2.0962	2.0941	2.0866	2.0781	2.0688	2.0662		2.0552		2.0390
15	0.0122	1	529.2	2.1254	2.1244	2.1199		2.0963	2.0915	2.0894		2.0734		2.0616	2.0555	2.0506	2.0354	2.0345
14	0.0146	1	492.1	2.1088	2.1078	2.1034		2.0802	2.0754	2.0733		2.0576		2.0459	2.0400	2.0351	2.0202	2.0193
13	0.0149	2	487.3	2.1066		2.1013	2.0970	2.0781	2.0733		2.0639		2.0465	2.0439	2.0380		2.0182	2.0173
12	0.0163	3	469.2	2.0986	2.0977		2.0891		2.0656	2.0635	2.0562	2.0480	2.0389	2.0364		2.0257		2.0100
11	0.0167	1	464.2	2.0964	2.0955	2.0911		2.0682	2.0634	2.0614		2.0459		2.0343	2.0284	2.0236	2.0088	2.0080
10	0.0186	4	441.6		2.0856	2.0813	2.0771	2.0585		2.0518	2.0446	2.0365	2.0275		2.0192	2.0144	1.9998	
9	0.0208	2	418.8	2.0767		2.0715	2.0673	2.0489	2.0443		2.0351		2.0182	2.0157	2.0095		1.9907	1.9898
8	0.0740	4	153.5		1.9674	1.9636	1.9598	1.9433		1.9373	**1.9308**	**1.9236**	**1.9156**		**1.9082**	**1.9039**	1.8908	
7	0.0756	1	149.5	1.9667	1.9658	1.9620		1.9418	1.9376	1.9358		**1.9221**		**1.9119**	**1.9067**	**1.9025**	1.8894	1.8886
6	0.0768	3	146.0	1.9653	1.9645		1.9569		1.9363	1.9345	**1.9280**	**1.9208**	**1.9129**	**1.9106**		**1.9012**		1.8874
5	0.0858	2	123.0	1.9565		1.9519	1.9482	1.9318	1.9277		**1.9195**		**1.9045**	**1.9023**	1.8971		1.8800	1.8792
4	0.1186	3	55.4	1.9309	1.9301		1.9229		1.9029	1.9012	1.8949	1.8880	1.8803	1.8781		1.8690		1.8556
3	0.1267	1	41.8	1.9259	1.9251	1.9214		1.9020	1.8980	1.8963		1.8831		1.8733	1.8684	1.8643	1.8517	1.8510
2	0.1512	2	5.0	1.9123		1.9079	1.9044	1.8888	1.8848		1.8770		1.8626	1.8605	1.8556		1.8392	1.8384
1	0.1543	2	0.9	1.9108		1.9064	1.9029	1.8873	1.8834		1.8756		1.8612	1.8591	1.8542		1.8378	1.8371

Fig. 2. Energy (cm^{-1}), Boltzmann occupation factors, selection rules and transition wavelengths of $^5I_7$ and $^5I_8$

In Fig. 2, for the 17 Stark split levels of the $^5I_8$ manifold and 15 ones of $^5I_7$ manifolds, their Boltzmann occupation factors, selection rules for electric dipole–dipole transitions Γ, energy (cm^{-1}) and all possible transition wavelengths are listed. The 17 and 15 energy levels were named using the numbers 1~17 or letters A~O respectively. For example, the letter "A" stood for the lowest energy level of $^5I_7$ manifold, and its energy is 5234.2 cm^{-1}, Boltzmann occupation factor is 0.1024 at 300 K and Γ is 4. The "17" stood for the highest upper level of $^5I_8$ manifold with the energy of 545.6 cm^{-1}, Boltzmann occupation factor of 0.0113 at 300 K and the Γ of 4. The data in the intersection cells of the vertical columns A~O and horizontal

Optics EXPRESS

rows 1~17 were the potential transition wavelengths between the Stark splitting levels of $^5I_7$ manifold and the Stark splitting levels of $^5I_8$ manifold. As shown in Fig. 2, the transition between the "A" level and the "17" level was forbidden because of the same parameter $\Gamma = 4$, while the data of 2.1254 μm meant the transition was permitted between the "A" level and "15" level with the different Γ of 4 and 1, respectively [15].

Filling the cells with different colors, all of the possible transitions in the range of I~II absorption bands and III~VI emission bands are shown in Fig. 2. And the energy level diagram had been shown in Fig. 3(a), respectively. There were several rules about the transitions for an in-band-pumped Ho:LuAG laser:

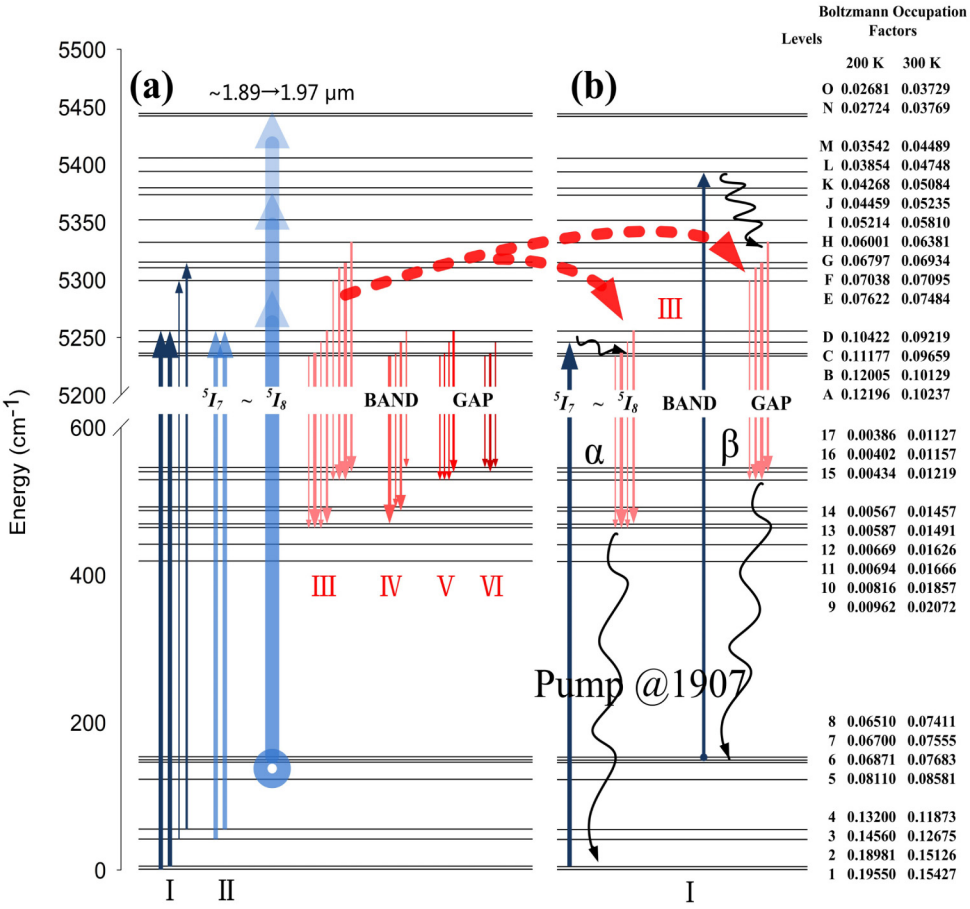

Fig. 3. Energy levels and potential transitions of Ho:LuAG: (a) absorption bands (I and II) and emission bands (III, IV, V and VI) ; (b) 1907 nm in-band-pump energy level systems consist of 2 groups of transitions: α and β.

1. The total populations of the 1~4 and 5~8 levels were ~0.5510 and ~0.3122 at 300 K respectively. The transitions from 1~8 levels of $^5I_8$ manifold to A~O levels of $^5I_7$ manifold dominated the absorption of an in-band-pump Ho:LuAG laser.

2. The transition wavelengths from 1~4 levels to $^5I_7$ manifold were about from 1837 to 1931 nm (in the 4 bottom rows of Fig. 2). Those from 5~8 levels to $^5I_7$ manifold were about from 1879 to 1967 nm. There were many possible alternatives as the in-band-pump wavelengths, such as, 1907, 1930, ~1880 and ~1965 nm. However, the absorption band from 1830 to 1900 nm was mainly due to the transitions from 1~4 levels to $^5I_7$ manifold, without commercially available pump sources. The absorption

Optics EXPRESS

band from 1934 to 1967 nm was mainly due to the transitions from 5~8 levels to $^5I_7$ manifold, and a wavelength tunable Tm fiber laser was an available pump source.

3. For the I~II absorption bands (~1900 to 1934 nm) in this paper, the contribution of the transitions from 5~8 levels to H~M levels was less than from 1~4 levels to A~D levels, in general, resulting from a small population of 5~8 levels.

4. The transitions from A~O levels to 9~17 levels dominated the emission bands, corresponding to the emission bands from ~1990 to 2132 nm.

5. In the III~VI emission bands (~2085 to 2150 nm), Ho:LuAG laser material had several emission peaks with the larger emission cross sections. The transitions from A~D levels to 11~17 levels were a major contributor for the III~VI emission bands. In the intersection cells of the A~D columns and 11~17 rows, the 21 data stood for the 21 potential emission wavelengths.

6. Above 2098 nm, the IV~VI laser emission bands with three peaks of 2101.0, 2124.7 and 2130.0 nm, were mainly affected by the transitions from the A~D levels to 12~17 levels. The III emission band of ~2094.5 nm center wavelength involved too many energy levels in the transitions, which could be divided into 2 groups. One group of transitions was from A~D levels to 11~13 levels and the other was from E~H levels to 15~17 levels. Both of them were shown in Fig. 2 with a yellow background. The 2 groups of transitions corresponded to 2 groups of laser energy level systems ["α" and "β" level systems shown in Fig. 3(b) and Table 1]. Considering the populations and energy differences of "α" and "β" level systems, they would show different lasing performances and emit slightly different laser wavelengths.

A knowledge of the energy levels and their transitions should be studied carefully before a Ho laser is established because that laser wavelengths maybe change under different operation circumstances, such as, shifting CW to Q-switched operation state without any other conditions changed, changing the transmittance of OCs, inserting an optical element and even only increasing pumping power. According to Fig. 2 and Fig. 3, some performance of a Ho:LuAG laser can be predicted.

Table 1. "α" and "β" level systems (Pumped by a narrow line-width 1907 nm Tm fiber laser).

Laser Level Systems	Absorption Band (I Band)			Emission Band (III Band)		
	Ground State Levels	Pump Band Levels	Transitions (Wavelengths (nm))	Upper Laser Levels	Lower Laser Levels	Potential Transitions (Wavelengths (nm))
α	1, 2	C	1→C (1906.4) 2→C (1907.9)	A~D	11~13	A→11 (2096.4) B→11 (2095.5) B→12 (2097.7) C→11 (2091.1) D→12 (2089.1) D→13 (2097.0)
β	7, 8	L	7→L (1906.7) 8→L (1908.2)	E~H	15~17	E→15 (2096.3) F→15 (2091.5) F→16 (2096.2) G→15 (2098.4) G→16 (2094.1) G→17 (2096.6) H→16 (2086.6) H→17 (2089.0)

As far as the pump sources are concerned at 300 K, many wavelengths can be chosen in the range of 1837~1967 nm but the absorption efficiency at 1907 nm is the highest. For a Ho:LuAG laser pumped by a ~1907 nm source, the absorption is mainly due to the transitions

Optics EXPRESS

from 1 and 2 levels to the C level, and the total population of 1 and 2 levels is ~0.3055 ("α" level systems shown in Fig. 3(b) and Table 1). It's also partly due to the transitions from 7 and 8 levels to the L levels, and the total population is ~0.1496 ("β" level systems shown in Fig. 2, Fig. 3(b), and Table 1). For ~1930 nm pump source, the total population of 4, 6 and 8 absorption levels is ~0.2694. Using the 1907 or 1930 nm pump sources, the higher E~H levels can be activated to produce the population inversions, assisting by phonon transition process. It is important to note that the H~M levels are higher levels compared to A~D level. This gives the Ho:LuAG laser a chance to emit the abundant potential wavelengths from ~2010 to ~2132 nm, corresponding to the transitions from A~M Stark splitting levels to the levels of $^5I_8$ manifold. So, some wavelengths beyond the III~VI emission bands can be obtained, such as a shorter wavelength of ~2077 nm [9]. Using a ~1.96 μm pump source, the transitions from the 5~8 levels to A~D levels can provide a lower quantum defect pumping mode to reduce thermal loading. However, shorter laser wavelengths are difficult to be achieved, such as ~2060 nm, because that Ho ions are difficult to jump up to the much higher levels than A~D levels only by phonon assisting, such as K level.

For the 1907, 1930 or ~1.960 nm pump sources, the absorption efficiencies of Ho:LuAG laser keep temperature sensitive. In Fig. 3(b), the data in the last two columns are the Boltzmann occupation factors at 200 and 300 K. When the temperature changes from 200 to 300 K, the populations of $^5I_8$ manifold are affected more than $^5I_7$ manifold. With the increase in temperature, the populations of 1~4 levels will decrease while that of 5~17 levels will increase as shown in Fig. 3(b). For a 1907 nm pump source, the increase in the populations of 7~8 levels is beneficial for forming "β" level systems: promoting more Ho ions from 7~8 levels to the L level and establishing population inversions from the E~G levels to 15~17 levels. However, for ~1907 nm pump source, with the increase of temperature, the absorption efficiency due to the transitions from 1 and 2 levels to the C level ("α" level systems) will reduce. So, with the increase in temperature, for the 1907 nm (also 1930 nm) pump sources, absorption efficiencies will decrease in general, but the more possible lasing wavelengths will be expected.

If only A~D levels as the upper levels of Ho:LuAG laser are excited by a 1907 or 1930 nm pump source and the phonon-assist process, which of the 21 potential wavelengths will be generated in a particular laser can be predicted by calculating the thresholds of the various transitions [13]. In [13], when a Ho ion is excited from the upper laser level to the lower laser level, the inversion reduction factor γ_e describes the change in the populations. Obviously, γ_e can be calculated with the Boltzmann occupation factors for a certain transition and is also temperature-sensitive. The value of γ_e for Ho is between 1.1 and 1.3, which is a quasi-four-level laser rather than a quasi-three-level laser. The emission cross sections in the IV~VI emission bands decrease in turn. Generally, a small round-trip loss corresponds to a long wavelength emitted in a CW Ho:LuAG laser and therefore the longest wavelength of ~2130 nm is expected when the laser loss is very low [22]. However, ~2095 nm wavelength is difficult to be predicted because that III emission band consists of the emission transition wavelengths of "α" and "β" level systems. If the laser loss is low, the transition wavelengths corresponding to "α" level systems will compete with IV~VI emission bands. If the laser loss is high, the transition wavelengths corresponding to "β" level systems will join in. Although the overall emission cross section of III band is similar to IV band at 300 K (shown in Fig. 1(b)), we estimate the emission cross section corresponding to "α" level systems is smaller than that of IV band (center wavelength: ~2101.0 nm), and more similar to V band (center wavelength: ~2124.7 nm). This can be deduced from the III and V emission cross sections became more same when the temperature was changed from 300 K to 80 K [6]. The emission wavelengths of "α" and "β" level systems are slightly different. In our earlier research, we found the round trip loss of Ho:LuAG laser was not large enough to promote Ho ions to the higher upper levels [5], so we used an uncoated Ho:LuAG to introduce a large insertion loss.

Optics EXPRESS

3. Experimental setup

The setup consisted of a plane pump coupling mirror (IC) and a plano-concave OC. The IC was coated with high reflectivity (> 99.8%) at the wavelength range of 2050-2250 nm and high transmission (> 98%) at the pump wavelength of 1850-1960 nm. The OCs (100 mm radius of curvature) were coated with a high reflectivity at 1850-1960 nm to reflect the unabsorbed pump power back into the medium for the second absorption. The transmissions of different OCs are 6, 10 or 20% at 2000-2250 nm. A ~13.2 mm long Ho:LuAG ceramic rod was wrapped with indium foil and mounted on a water-cooled copper heat sink maintained at ~15 °C. The Ho:LuAG ceramic laser medium with a doping concentration of 1 at.% was developed by a reactive sintering method under vacuum. The pump source was a tunable Tm fiber laser which consisted of a ~3 m long and double-clad fiber with a 25 μm diameter Tm-doped core (0.17 NA) surrounded by a 300 μm diameter pure silica inner cladding (0.49 NA). The wavelength of the fiber laser was tuned to match the Ho:LuAG absorption peak at ~1907 nm with a narrow band-width (< 1nm, FWHM). The physical length of the resonator was ~18 mm, and the focusing lens were tuned to achieve the mode matching.

4. Results and discussion

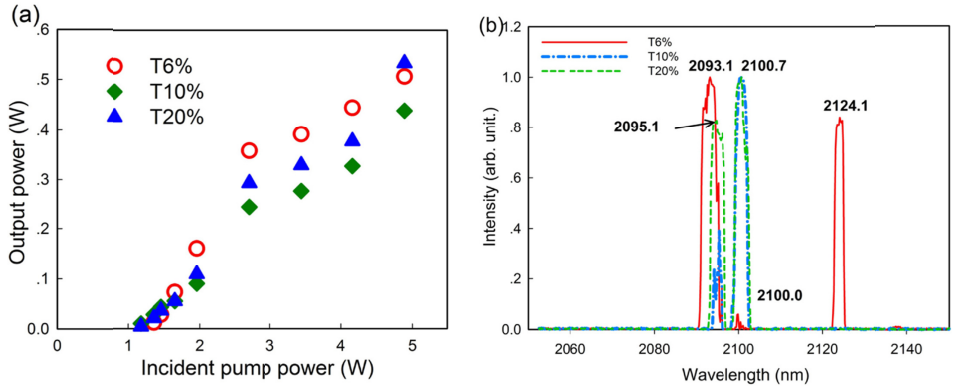

Fig. 4. Output power versus incident pump power (a) and emission spectrum for different OCs of 6, 10 and 20% transmissions(b).

When the OCs of T = 6, 10 and 20% were used, the laser had almost the same threshold power of ~1 W and output power of ~0.5 W under an incident pump power of ~4.9 W (shown in Fig. 4(a)). The emission spectrum was analyzed using an optical spectrum analyzer (AQ6375, Yokogawa) and shown in Fig. 4(b). With the 6% output coupler, three emission bands were observed and the center wavelengths were 2093.1, 2124.1 and ~2100.0 nm. Although the 2100.0 nm emission was very weak, it could still be distinguished. For the OCs of T = 10% or 20%, twin wavelengths were both observed and the center wavelengths shifted to ~2095 and ~2101 nm. With the increase in the transmissions of OCs, it was obvious that the emission spectrum shifted toward the short wavelength range

For a Ho:LuAG laser, Ho ions must be pumped to the upper laser energy levels fast enough to produce the population inversion between upper and lower energy levels. Furthermore, the pumping power must overcome the laser losses. When the candidate laser transitions in Fig. 2 overcame their thresholds, their corresponding laser wavelength would be emitted. Without the antireflection coatings, the Ho:LuAG ceramic laser medium introduced an insertion loss of ~0.298 to the laser, due to the Fresnel reflection. More Ho ions are promoted up to the $^5I_7$ manifold to overcome laser thresholds. This result served to activate more upper energy levels to establish laser level systems and produce the population inversions, such as E~H levels. Furthermore, when more Stark splitting levels of the $^5I_7$

Optics EXPRESS

manifold were activated, twin or multi- wavelengths might be obtained. Nevertheless, if the round trip loss was not large enough, the transitions from A~D levels to $^5I_8$ manifold would dominate the laser emission, the wavelengths of which were mainly confined in the 21 data as mentioned earlier.

In Fig. 4(b), each of emission bands was wide enough to consist of several possible energy transition wavelengths. For the OC of T = 6%, there were three emission bands at the range of from 2091.0 to 2095.1 nm (part of III, the same below), 2123.0 to 2125.3 nm (V) and 2099.5 to 2100.5 nm (IV). This meant that A~D energy levels and 11~17 energy levels were activated to form level systems, as the laser upper and lower levels respectively. As the laser emission bands were discontinuous, some but not all of 21 potential laser transitions in Fig. 2 made a contribution to the laser operation. With a center wavelength of 2093.1 nm, the emission band from 2091.0 to 2095.1 nm (III) was due to the transitions of the "α" level systems, corresponding to the B→11 and C→11 transitions. As the emission intensities of III ("α" level systems) and V bands were similar, we believed the emission cross section of "α" level systems was similar to that of V emission band, which was smaller than that of IV emission band.

With the increase of the transmissions of OCs, the laser round trip losses turned to increase. For the OC of T = 10%, the emission intensity at ~2095 nm was much weaker than that of ~2101 nm. Using the OC of T = 10%, the V emission band vanished but the IV emission band emerged. The III emission band became weak and the center wavelength shifted to 2095.1 nm. This meant the transitions of the "α" level systems were gradually switched off and became weak with the increase of laser loss. The disappearing of V emission band accompanied by decaying of III ("α" level systems) proved again the emission cross section of "α" level systems was similar to that of V emission band.

Table 2. Several parameters of Ho:LuAG energy level transitions.

Sample		**1 at.% Ho:LuAG (Ref. 5)**		**1 at.% Ho:LuAG (this paper)**		
Antireflection coating		Yes		No		
T (%)		6	20	6	10	20
Loss (= -lnR)		0.062	0.223	0.062	0.105	0.223
Insertion loss		0	0	0.298	0.298	0.298
Total loss*		**0.062**	**0.223**	**0.360**	**0.403**	**0.522**
Number of emission bands		1 (V)	1 (IV)	3 (III, IV, V)	2 (III, IV)	2 (III, IV)
Emission range (nm)	III	/	/	2091.0 ~2095.1	2093.8 ~2095.8	2093.1 ~2096.5
	IV	/	2100.0 ~2102.2	2099.5 ~2100.5	2098.8 ~2102.3	2098.8 ~2102.3
	V	2123.3 ~2125.3	/	2123.0 ~2125.3	/	/
Center wavelength (nm)	III	/	/	2093.1	2095.1	2095.1
	IV	/	2100.7	2100.0	2100.7	2100.7
	V	2124.5	/	2124.1	/	/
Possible emission transitions	III	/	/	B→11 (α) C→11 (α)	B→11 (α) G→16** (β)	A→11 (α) B→11 (α) D→13** (α) E→15 (β) F→16 (β) G→16 (β) G→17 (β)
	IV	/	A→12** C→13	C→13	A→12 C→13	A→12 C→13
	V	A→15 B→15 D→17	/	A→15 B→15 D→17	/	/

*: Without intrinsic losses **: Uncertain transition

Optics EXPRESS

For the OC of T = 20%, the III emission band became strong again and almost similar to IV emission band. However, the range of the emission band slightly shifted to the long wavelengths region from 2093.1 to 2096.5 nm as shown in Fig. 4(b). This meant the "β" level systems joined in the transitions at least. The higher levels E, G and H were activated to contribute the lasing performance, such as, E→15, F→16 and G→17. All of above transitions and the evolutions of transitions were shown in Table 2.

Furthermore, in our earlier research [5], using the same Ho:LuAG ceramic medium with an antireflection coating, only a narrow emission band was achieved for both of T = 6% and 20% OCs, with a center wavelength of 2124.5 (V) or 2100.7 nm (IV) respectively. Narrow emission bands meant only a few transitions from the A~D levels to $^5I_8$ manifold were activated. In [5], laser wavelength blue shift was also observed when T turned from 6% to 20%. The data in Table 2 may help us to understand the transitions of the Ho:LuAG medium and the wavelengths can be predicted roughly at least.

5. Conclusion

The energy level structure of Ho:LuAG (as well as Ho:YAG) was very extraordinary. There were 192 potential transitions between 17 Stark splitting energy levels of $^5I_8$ manifold and 15 ones of $^5I_7$ manifold, covering a broad wavelength range from 1837 to 2132 nm. The energy gaps of some Stark splitting levels were too small to distinguish their differences of lasing performance, particularly, when phonon assist process joined in. Several absorption peaks of 1900~1934 nm absorption band, such as ~1907 and ~1930 nm, benefited from the abundant potential transitions and had larger absorption cross sections. In general, absorption peaks result from the combination effect of several different absorption transitions, which have different ground state and pump band levels. Emission bands played the same rules. Ho:LuAG laser became very interesting because it had the similar absorption and emission wavelengths but implied different laser energy level systems.

For a Ho:LuAG laser in-band pumped by a narrow line-width Tm fiber laser, We believe the increase of laser threshold, such as, using a high-transmission OC and inserting an optical element, is conducive to achieving shorter wavelengths. We analyzed the potential transitions wavelength to form in-band-pumped level systems and found the III emission band consisted of "α" and "β" level systems. Each of them had a different group of upper and lower laser level which led to different laser performances. Using three different transmission OCs and an uncoated Ho:LuAG ceramic medium to introduce losses, almost the same ~0.5 W output power was obtained under ~4.9 W pump power. With the increase of round trip loss, different levels joined in the laser operation in order. This transition evolution proved the absorption cross section of "α" level systems (part of III emission band) is similar to that of ~2124 nm absorption band (V). From Fig. 2, a short wavelength, such as ~2077 nm, will be predicted when a hundred-watt output power Ho:LuAG laser is performed which in general need a high transmission OC.

There are so many potential transitions in Ho:LuAG laser (as well as Ho:YAG) that we should be very careful about designing an in-band-pumped Ho laser, especially the wavelengths needing to be locked. The wavelengths of pump sources will have a great effect on forming the laser energy level systems. Compared to Ho:YAG laser material, the energy levels and laser transitions of Ho:LuAG have some slight differences. The Ho doped YAG and LuAG mixed ceramic laser medium is expected because it may have more abundant laser transitions and a wider spectrum range.

Funding

National Natural Science Foundation of China (NSFC) (11274144, 51302115, 51402133, 61177045, U1430111); Priority Academic Program Development of Jiangsu Higher Education Institutions (PAPD).